

REPORT DOCUMENTATION PAGE

AFRL-SR-BL-TR-00-

Public reporting burden for this collection of information is estimated to average 1 hour per response, gathering and maintaining the data needed, and completing and reviewing the collection of information, including suggestions for reducing this burden, to Washington Headquarters Collection of information, including suggestions for reducing this burden, to Washington Headquarters Davis Highway, Suite 1204, Arlington, VA 22202-4302, and to the Office of Management and Budget

ita sources,
pect of this
5 Jefferson
33.

1. AGENCY USE ONLY (Leave blank)		2. REPORT DATE March 2000	3. REPORT TYPE AND DATES COVERED Final Technical Report 1 Apr 97 to 30 Sep 99
4. TITLE AND SUBTITLE Theoretical Aerodynamics Research			5. FUNDING NUMBERS F49620-97-1-0141
6. AUTHOR(S) Julian D. Cole & Oleg S. Ryzhov			
7. PERFORMING ORGANIZATION NAME(S) AND ADDRESS(ES) Department of Mathematical Sciences Rensselaer Polytechnic Institute Troy, NY 12180-3590			8. PERFORMING ORGANIZATION REPORT NUMBER
9. SPONSORING/MONITORING AGENCY NAME(S) AND ADDRESS(ES) AFOSR/NM 801 N. Randolph St, Rm 732 Arlington, VA 22203-1977			10. SPONSORING/MONITORING AGENCY REPORT NUMBER F49620-97-1-0141
11. SUPPLEMENTARY NOTES			
12a. DISTRIBUTION AVAILABILITY STATEMENT Approved for public release; distribution unlimited.			12b. DISTRIBUTION CODE
13. ABSTRACT (Maximum 200 words) <p>The blunted-nose high-pressure drag is shown to exert great impact on the hypersonic flow field even in the strong interaction regime governed by viscous effects. This impact vanishes downstream where the viscous/inviscid interaction becomes dominant.</p> <p>Optimization of conical wings in hypersonic flight substantially reduces the wave drag. A pertinent figure of merit $F = CD/CL^{3/2}$ decreases by more than 4%.</p> <p>The concept of absolute instability in the streamwise and crossflow directions is a breakthrough in our understanding of boundary-layer properties on swept wings and gas-turbine blades where the flow field is highly three-dimensional. Many contradictions in this area were building up for decades and eventually cast doubts on the very validity of hydrodynamic stability theory. No reliable transition-prediction methods could exist on this basis. New methods to be developed in place of those used currently must incorporate the possibility of earlier transition due to upstream advancing wave packets.</p>			
14. SUBJECT TERMS			15. NUMBER OF PAGES
			16. PRICE CODE
17. SECURITY CLASSIFICATION OF REPORT UNCLASSIFIED	18. SECURITY CLASSIFICATION OF THIS PAGE UNCLASSIFIED	19. SECURITY CLASSIFICATION OF ABSTRACT UNCLASSIFIED	20. LIMITATION OF ABSTRACT UL

Final Report on Theoretical Aerodynamics Research (Grant F49620-97-1-0141)

by

Julian D. Cole & Oleg S. Ryzhov
Rensselaer Polytechnic Institute

A premature death of Professor Julian D. Cole in April 1999 ended the successful work on this project designed for three years. However, the progress made by that time covered the major topics that had been included in the proposal.

Objectives

Research sponsored under the grant consists of two parts:

- i) Blunted-nose effects and wings of optimal shapes in hypersonic flight
- ii) Swept-wing boundary-layer instabilities

Accordingly, the project objectives are two-fold:

- i) To evaluate the blunted-nose high-pressure drag in the strong interaction regime and determine conical wing shapes that minimize wave drag for a given lift, fixed by technological requirements, in steady hypersonic flights
- ii) To revise hydrodynamic stability theory, as applied to three-dimensional boundary layers on swept wings and gas-turbine blades, on the basis of absolute instability that evolves in any of two orthogonal directions.

Hypersonic Aerodynamics

The framework for this topic is ideal, inviscid flow with the additional assumption that the body is thin and at a small angle of attack so that the velocity and pressure fields can be described by the equations of hypersonic small-disturbance (HSD) theory. This theory provides a similarity law in which the high free-stream Mach number M_∞ and a measure of flow deflection δ are combined into a single parameter $H=(M_\infty\delta)^2$, thereby essentially reducing the amount of computational work.

Blunted-Nose Effects

A problem is posed to simulate the influence of the nose bluntness on the hypersonic flow field around a slender two-dimensional section shown in Figure 1. In the formulation used, a bow shock is given in advance whereas the body contour comes in the course of analysis being identified with a particular streamline. An equation for the shock shape involves two terms that specify the contributions from the strong viscous-inviscid interaction and the blunted-nose high-pressure inviscid drag.

20000420 155

Matched asymptotic expansions are used to solve the problem within the hypersonic small disturbance theory providing the framework for this part of research. In the outer region bounded by the shock, two sets of ordinary differential equations control the pressure, density and velocity distributions. One of these systems admits of an explicit integral that is associated with the finite drag exerted on the blunted nose of a section. The use of the momentum conservation law allows us to derive an integral in the closed form, thereby drastically simplifying a solution. Governing equations in the inner region occupied by a high-entropy layer are integrated, explicitly determining the influence of the blunted-nose effects on the flow field arising from the strong viscous/inviscid interaction.

A thorough analysis of the Newtonian approach reveals certain limitations inherent in this simplified treatment of steady hypersonic flows. However, a rigorous passage to the limit as $\gamma \rightarrow 1$ is exploited in Figure 2 to demonstrate extremely strong variations of a parameter A_3/B_1 , indicative of the pressure-to-velocity ratio at the section surface, for blunted-nosed bodies.

Optimum Wings

Wing designs are restricted to a conical geometry, which reduces the number of independent variables, while still producing practical wing shapes. The flow above the wing is assumed to be expansive so that the drag-to-lift performance of the wing is dominated by the compressive flow below the wing. A typical conical wing with zero thickness is shown in Figure 3 where $Y=y/x$, $Z=z/x$.

An optimization problem is solved for the compressive flow underneath wings at small incidence. The method chosen is a second-order, finite-volume, shock-capturing scheme. For a given wing shape, the flow underneath the wing is computed, and it is found that this computation can be performed to a high degree of accuracy independently of the flow above the wing, even for cases where the bow shock is detached from the body. Based on the HSD formulation, a figure of merit F is expressed in terms of the drag coefficient C_D and the lift coefficient C_L as $F=C_D/C_L^{3/2}$. The figure of merit is computed for each wing using a finite volume discretization of the HSD equations. A set of design variables that determine the shape of the wing is obtained and adjusted iteratively to find a shape that minimizes F for a given value of hypersonic similarity parameter H and planform area. This procedure corresponds to a shape that minimizes the drag coefficient C_D for a fixed lift coefficient C_L . Once an optimum wing shape is found, the shock attachment or detachment is determined using a local analysis of the flow near the wing leading edge.

Optimum shapes are computed for flat delta wings and for a family of caret wings. In both cases, the wing design is improved iteratively with respect to the figure of merit toward an optimum. Quite unexpectedly, the optima have detached bow shocks for each of the flat delta wings studied.

An improved drag-to-lift performance is found using the optimization procedure for curved wing shapes. For the general class of wing shapes, a number of optimum designs are indicated. The bow shocks for all of these optimum wings prove to be attached, although some initial designs have detached shocks. Typically, but not always, the pressure along the

wing is nearly uniform. It is noted that the optima appear to be unique for a given planform area and a value for H , as indicated by numerical experiments in which several different initial shapes lead to the same wings that minimize wave drag. The work gives a powerful means for hypersonic aircraft design. Optimization procedure results in more than 4% reduction in $C_D/C_L^{3/2}$.

Work in progress by April 1999 on hypersonic wings had been planned to involve also a study of optimum planforms. This was intended to be carried out under the same hypersonic small-disturbance theory. The demise of Professor Julian D. Cole put an end to this research. The joint work with Professors Cook and Schleinger of Delaware on the disturbance pattern induced by a weak shock impinging on a thin wedge was stopped also.

Figure 4 presents the flow patterns for a cavet wing and two smooth optimized wings for the same value $H=2.0$ of the hypersonic similarity parameter. Figure 5 is a summary of smooth optima and the related flat wing which demonstrates the reduction of $C_D/C_L^{3/2}$ achieved through optimization.

Boundary-Layer Instabilities

Initially, the work on this topic was aimed at revising the current transition-prediction methods for swept wings of modern aircraft and drag recution. In the course of research it became clear that one more area of applications of vital importance is a gas-turbine blade operating with three-dimensional base flows. An acute need for the rigorous mathematical analysis stems from the fact that for many years (actually decades) the problem on the boundary layer on a swept wing was extremely controversial, involving contradictions between theory and experiment. What is worse, even experimentalists themselves could not reach a good consensus of opinion on findings from different wind tunnels and set-ups. So, the state of the art called (and stills calls) into question our knowledge of transition mechanisms and the e^N - method for prediction of transition.

To provide solid grounds for theoretical conclusions an asymptotic model for the wave motion in a steady three-dimensional subsonic boundary layer was developed on the assumption that the Reynolds number is high enough.

This generalized triple-deck model offers a clue to the eigen-value problem that describes eigenmodes of different nature, including Tollmien-Schlichting waves and crossflow vortices coupled together. The Reynolds number enters the final formulation where a high-order term in the interaction law depends on centrifugal forces due to the large curvature of stream-surfaces.

A receptivity problem on linear disturbances artificially excited in a three-dimensional boundary layer is solved in the framework of the generalized triple-deck theory. In order to derive a solution that simulates typical conditions in wind-tunnel tests and can be compared with experimental data, the base flow over a swept flat plate is considered. As in real measurements, crossflow in the boundary layer is supposed to originate o wing to almost constant pressure gradient induced from outside with a displacement body on top. In this formulation, the receptivity problem allows a rigorous analysis to be carried out without additional assumptions. Thus, the theoretical inferences are put on a firm footing.

The most striking result from the asymptotic theory is the discovery of absolute streamwise and crossflow instabilities intrinsic to three-dimensional boundary layers on swept wings and turbine blades at high Reynolds numbers. The results obtained point to the fact that wave packets of different kinds can be generated by an external source operating in the pulse mode (vibrating ribbon in the wind-tunnel experiments, turbulent patches in flight, wakes from the upstream rows of blades in gas turbine engines). Rapidly growing wave packets sweep downstream; however, the formation of wave packets that move against the oncoming stream and crossflow is proved rigorously. Insofar as the amplitude of all of these modulated signals increases exponentially in time and space, the excitation process gives rise to absolutely unstable disturbances in an arbitrary direction provoking interactions of different eigenmodes and leading to earlier transition.

A rigorous proof to predict absolute instability relies on the so-called dispersion relation connecting the frequency and wave numbers of disturbances intrinsic to the crossflow component of velocity. Careful investigation of the complex frequency plane disclosed the existence of a specific eigenmode that was not found in all previous analysis. This eigenmode is responsible for two additional lobes integrated into both branches of the dispersion curves in Figures 6 and 7. The fine structure of the dispersion curves depends on values of the streamwise and crossflow wave numbers. Figure 6 presents a typical behavior of the dispersion curve with moderate values of the crossflow wavenumber. The group velocity at the global maximum of $\text{Re}(\omega)$ labeled "g" is positive, whereas it takes on a negative value at a local maximum labeled "d". Figure 7 gives an idea of the shape of the dispersion curve with large values of the crossflow wavenumber. There remains the single global maximum of $\text{Re}(\omega)$ where the group velocity is positive.

Accordingly, the wavepacket shown in Figure 8 for moderate values of the crossflow wavenumber is associated with the global maximum "g" in Figure 6. The highly modulated disturbance of this type sweeps downstream giving rise to convective instability, characteristic of a two-dimensional boundary layer, and a conventional route to transition. However, regardless of the values of both wavenumbers the disturbances become capable of moving ahead of an outer perturbing source as illustrated by Figures 9 and 10. The most dangerous for the laminar state of a boundary layer is the wavepacket in Figure 9 triggered by the local maximum of $\text{Re}(\omega)$ labeled "d" in Figure 6; this wave packet propagates against the direction of the oncoming stream. A different scenario takes place in the case of large values of the crossflow wavenumber. Figure 10 shows the wavepacket induced by the dispersion curve in Figure 7. The disturbance as a whole moves downstream, however, the long-wavelength oscillation cycles at its tail end penetrate the region upstream of the perturbing source where they enhance exponentially.

The special computation confirms the discovery of the upstream advancing signals. Wave packets of both types may provoke much earlier transition to turbulence. The route to transition with the underlying mechanism of absolute instability at the bottom has been completely ignored so far.

The results achieved are shown broadly consistent with wind-tunnel measurements and numerical findings. They uncover the root of many controversial issues in current studies of three-dimensional boundary-layer instabilities.

Accomplishments

The blunted-nose high-pressure drag is shown to exert great impact on the hypersonic flow field even in the strong interaction regime governed by viscous effects. This impact vanishes downstream where the viscous/inviscid interaction becomes dominant.

Optimization of conical wings in hypersonic flight substantially reduces the wave drag. A pertinent figure of merit $F=C_D/C_L^{3/2}$ decreases by more than 4%.

The concept of absolute instability in the streamwise and crossflow directions is a breakthrough in our understanding of boundary-layer properties on swept wings and gas-turbine blades where the flow field is highly three-dimensional. Many contradictions in this area were building up for decades and eventually cast doubts on the very validity of hydrodynamic stability theory. No reliable transition-prediction methods could exist on this basis. New methods to be developed in place of those used currently must incorporate the possibility of earlier transition due to upstream advancing wave packets.

Future Development

The mechanism of absolute instabilities seems to be also at the heart of the self-sustained production of large near-wall coherent structures in turbulent flows. A recent experimental model advanced by Professor R. Blackwelder (University of Southern California) starts from a close analogy between the near-wall turbulent streaks and Görtler vortices on a concave surface. If so, then establishing a rigorous mathematical link between the three-dimensional Tollmien-Schlichting waves and Görtler vortical patterns become of principal significance. Up to now the Görtler vortices were believed to be completely dissimilar to the Tollmien-Schlichting eigenmodes studied in detail both theoretically and experimentally. Besides, on the concave part of the lower gas-turbine-blade surface the Görtler instability can be a dominant factor leading to transition.

The work on absolute instability developing in an arbitrary direction was interrupted in April 1999 and resumed at the University of California, Davis in August 1999 under the new grant F49620-00-1-0066. The main issue to be resolved is that the same basic mechanisms take place in the general case and are intrinsic also to the Görtler vortices.

It might be well to emphasize that an extensive work on absolute instability and related problems of separation is in progress in Europe. In Germany, it is carried out at DLR Institut für Strömungsmechanik, Göttingen. In England research at the famous Department of Applied Mathematics and Theoretical Physics, Cambridge University is supported by British Aerospace Aerobus, Ltd.

Papers Published

Hypersonic Aerodynamics

Blunted-Nose Effects

1. Ryzhov, O. S., Cole, J. D. and Malmuth, N. D., 1996, On a blunt-body problem in hypersonic flow theory. AIAA Paper 96-2151.
2. Ryzhov, O. S., Cole, J. D. and Malmuth, N. D., 1998, A blunt-nosed thin body in hypersonic flow. *SIAM Journal of Applied Mathematics*, 58, 345-369.

Optimum Wings

3. Triantafillou, S. A., Schwendeman, D. W. and Cole, J. D., 1998, Optimization of conical wings in hypersonic flow. *Theoretical and Computational Fluid Dynamics*, 12, 219-232.

Boundary-Layer Instabilities

4. Ryzhov, O. S. and Terent'ev, E. D., 1996, A composite asymptotic model for the wave motion in a steady three-dimensional boundary layer. *Journal of Fluid Mechanics*, 337, 103-128.
5. Ryzhov, O. S. and Terent'ev, E. D., 1998, Streamwise absolute instability of a three-dimensional boundary layer at high Reynolds numbers. *Journal of Fluid Mechanics*, 373, 111-153.
6. Ryzhov, O. S., Cole, J. D. and Malmuth, N. D., 1998, Excitation of convectively and absolutely unstable disturbances in three-dimensional boundary layers. AIAA Paper 98-2861.
7. Ryzhov, O. S. and Terent'ev, E. D., 1998, Excitation of absolutely unstable disturbances in boundary layer flows. In *Frontiers of Computational Fluid Dynamics*, 1998. World Scientific.

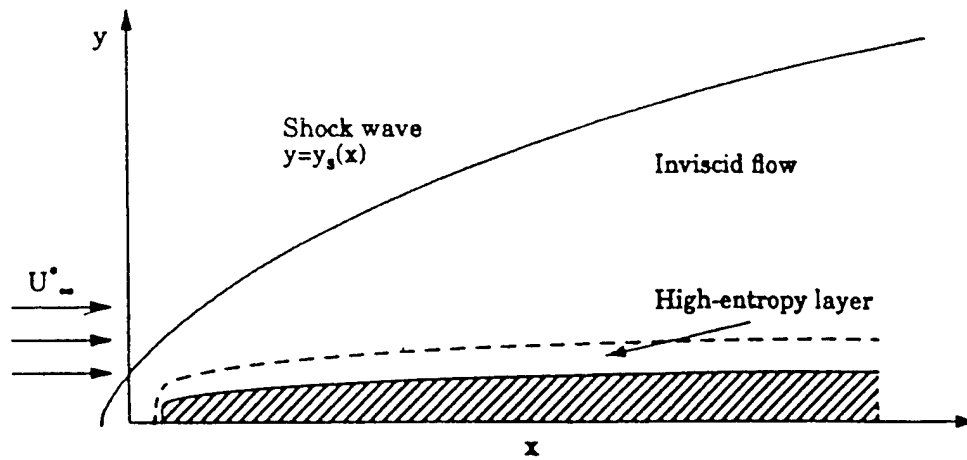


Figure 1. Inviscid supersonic flow past a two-dimensional section simulating the combined influence of the nose bluntness and a boundary layer adjacent to the body surface.

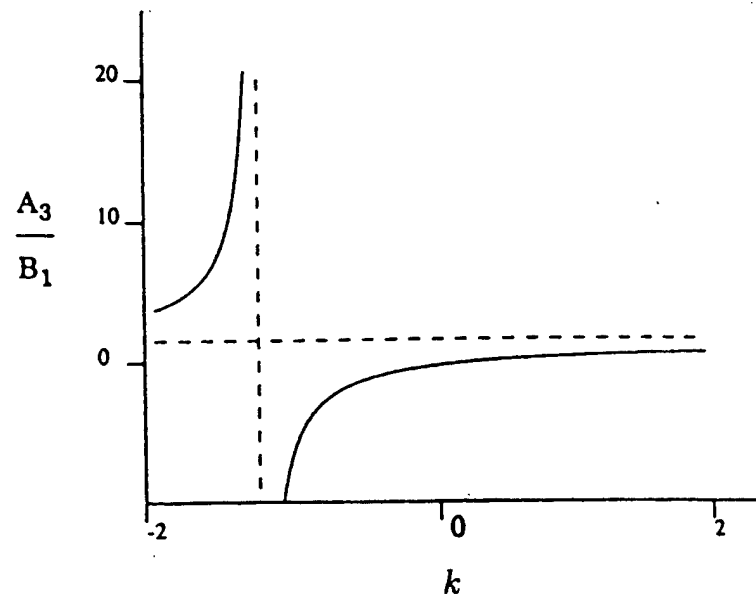


Figure 2. A ratio A_3/B_1 as a function of a parameter k used in a passage to the limit as $\gamma \rightarrow 1$. A value $k=0$ giving $A_3/B_1 = -\frac{2}{3}$ is associated with the energy conservation law.

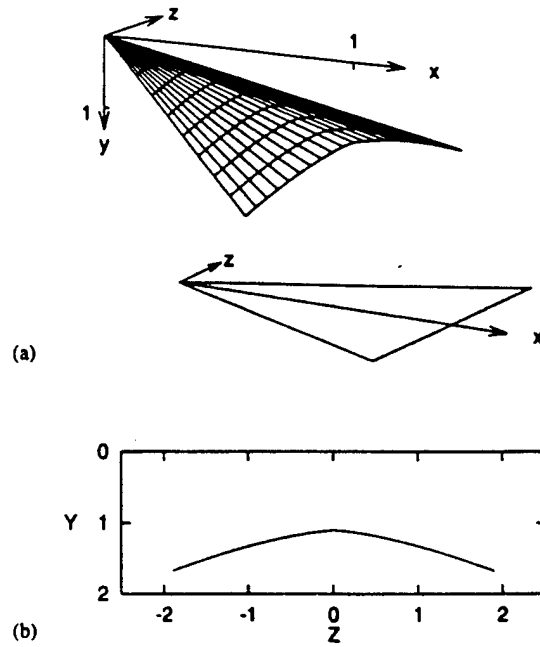


Figure 3. Conical wing: (a) shape and planform and (b) projection in conical (Y, Z) – plane.

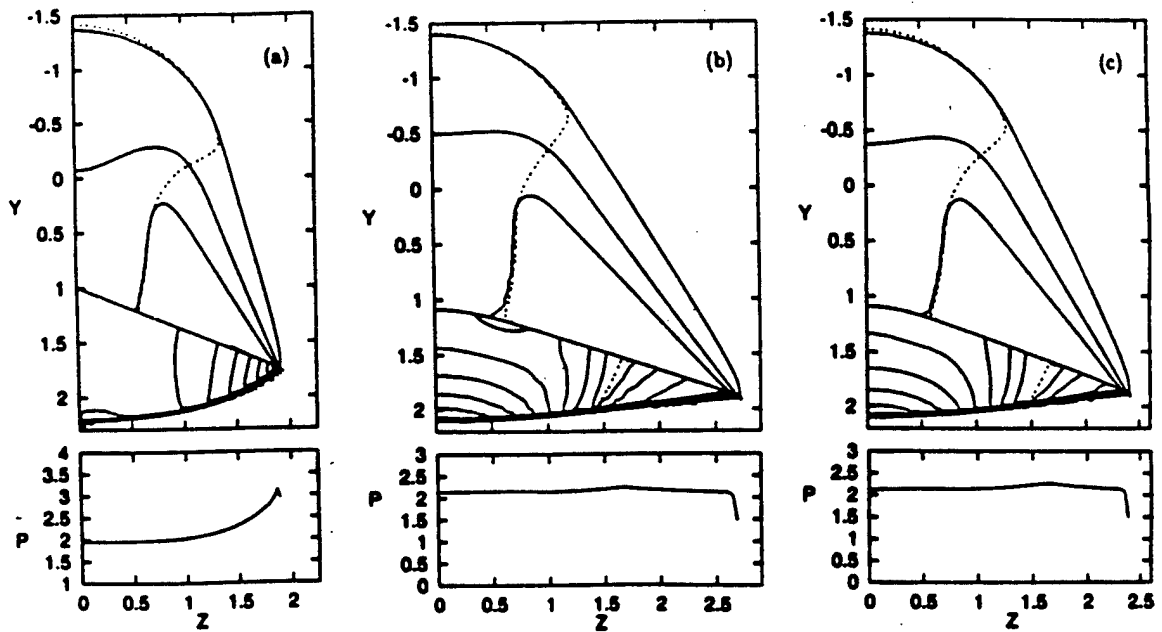


Figure 4. Flow results for: (a) caret wing with $H = 2.0$, $\Lambda = 1.9$, $W(\Lambda) = 1.75$; (b) smooth optimized wing with $H = 2.0$, $\Lambda = 2.7$; (c) smooth optimized wing with $H = 2.0$, $\Lambda = 2.4$. Upper plots show pressure contours and lower plots pressure on lower surface.

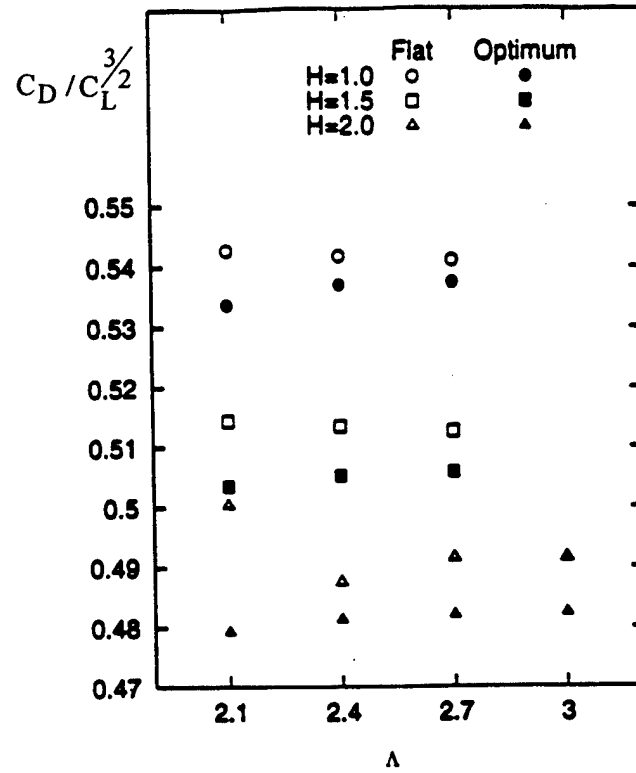


Figure 5. Summary of smooth optima and related flat wings which demonstrate reduction in $C_D / C_L^{3/2}$.

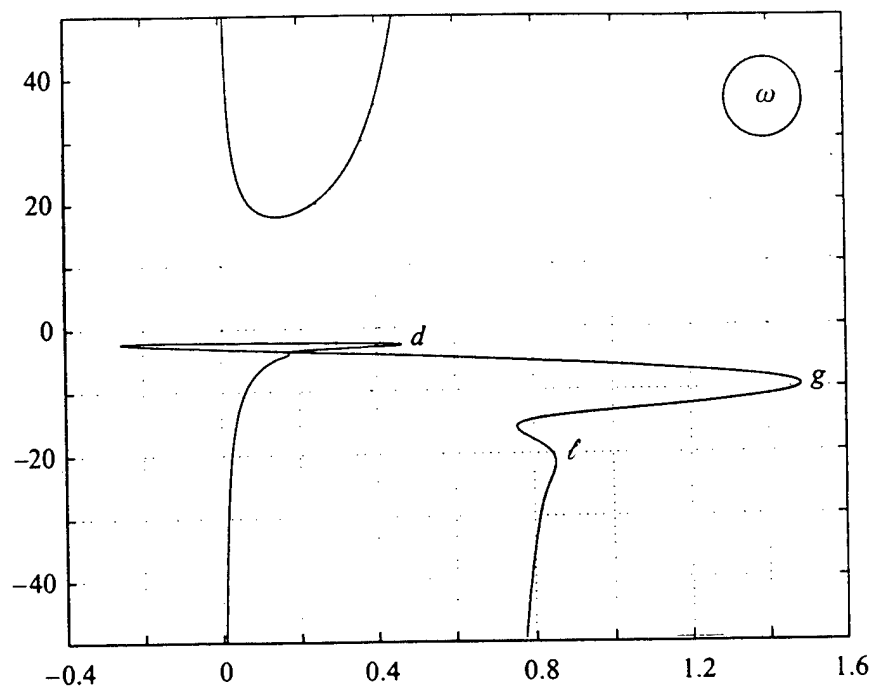


Figure 6. Typical behavior of the dispersion curve in the complex frequency plane ω with moderate values of the crossflow wavenumber. A loop with a local maximum of $\text{Re}(\omega)$ labeled "d" is formed on the lower branch.

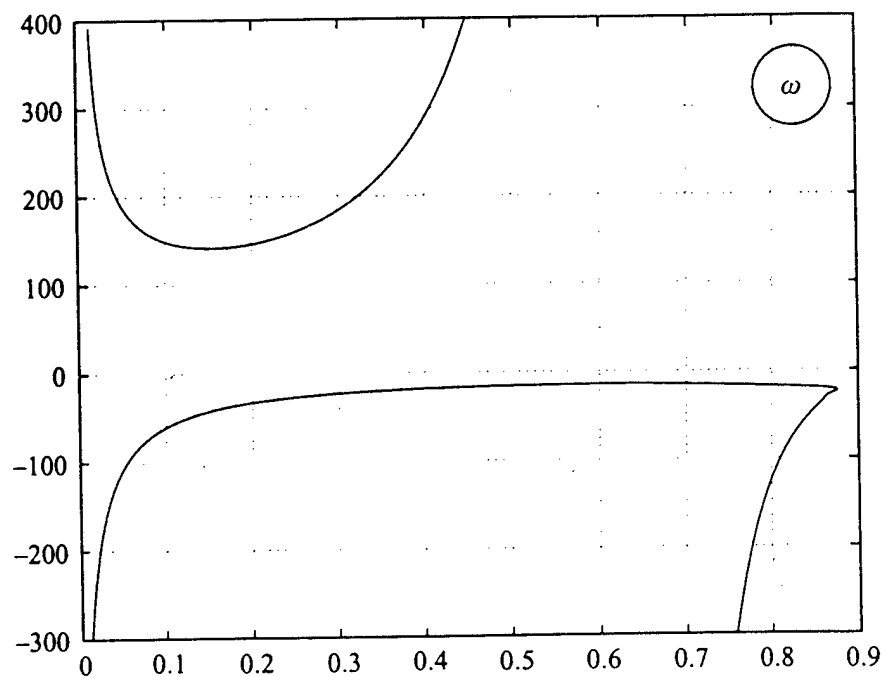


Figure 7. Typical behavior of the dispersion curve in the complex frequency plane ω with large values of the crossflow wavenumber. The loop disappears from the lower branch where there remains the single global maximum of $\text{Re}(\omega)$.

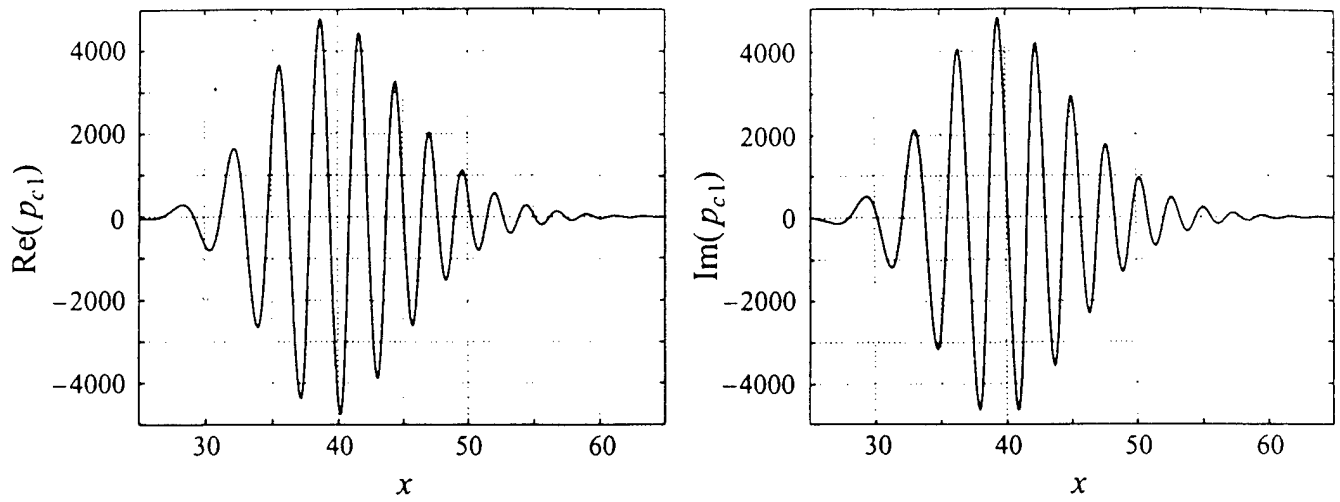


Figure 8. Downstream sweeping wave packet induced by the global maximum "g" of $\text{Re}(\omega)$ in Figure 6.

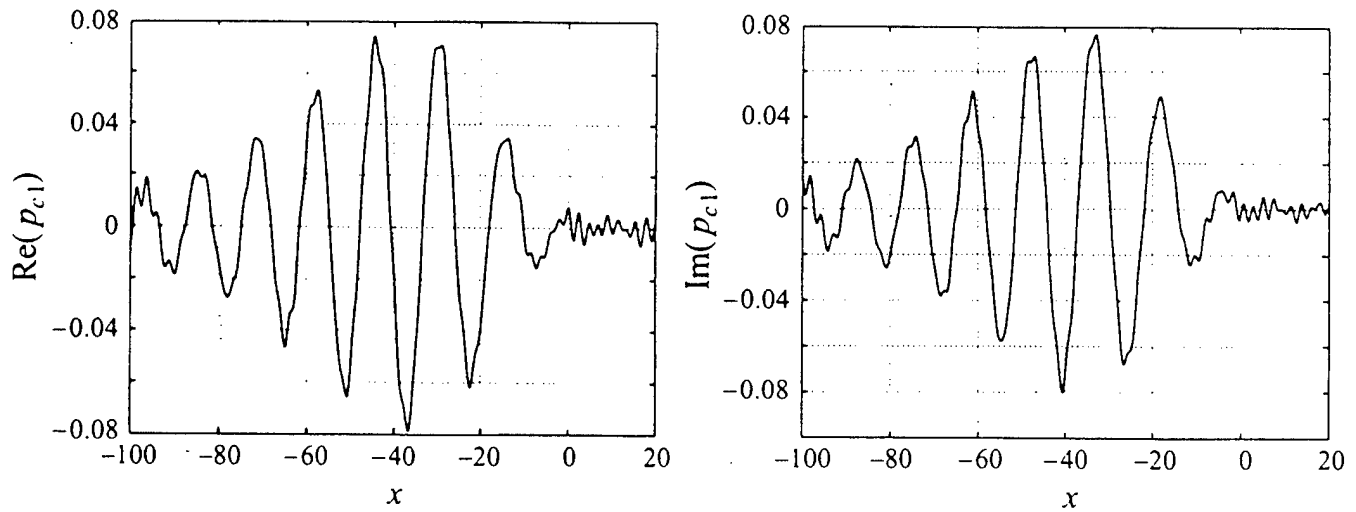


Figure 9. Upstream advancing wave packet induced by the local maximum "d" of $\text{Re}(\omega)$ in Figure 6.

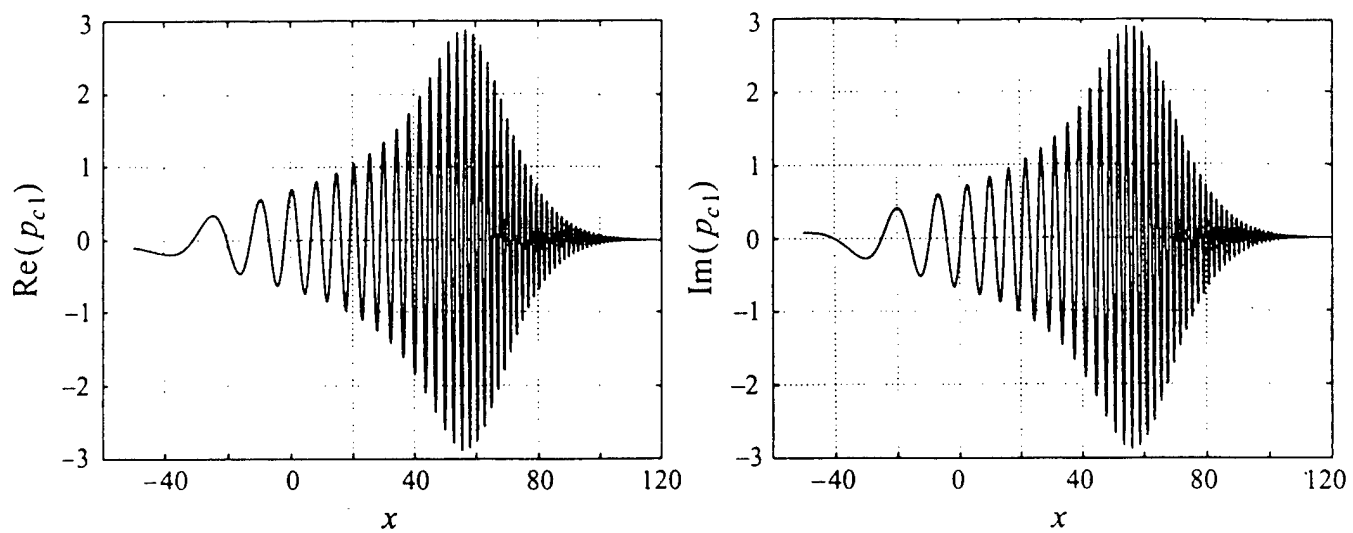


Figure 10. Single indivisible wavepacket triggered by the dispersion curve in Figure 7.